Polymer Chemistry

Accepted Manuscript

This article can be cited before page numbers have been issued, to do this please use: M. Skala, Q. Ye, A. P. Kitos Vasconcelos, K. A. Polich, S. Narayan-Sarathy and M. Golder, *Polym. Chem.*, 2026, DOI: 10.1039/D6PY00436A.

ROYAL SOCIETY OF CHEMISTRY

rsc.li/polymers

View Article Online
DOI: 10.1039/D6PY00436A

Tunable Dynamic Covalent Networks from Mechanochemical Depolymerization of Post-Consumer Aliphatic Polyesters

Morgan E. Skala,[1] Qian Ye,[1] Ana Paula Kitos Vasconcelos,[1] Katie A. Polich,[1] Sridevi Narayan-Sarathy,[2] and Matthew R. Golder*[1]

[1] Department of Chemistry and Molecular Engineering & Science Institute
University of Washington, Seattle, WA 98195

[2]PepsiCo Foods Packaging R&D – Sustainability,
Plano, TX 75024

Abstract: Aliphatic polyesters such as poly(lactic acid) (PLA) and poly(hydroxyalkanoates) (PHAs) are inherently biodegradable, therefore these materials are typically collected and composted at end of life which results in products that prevent recycling and repurposing into new materials. Chemical recycling presents an orthogonal method for the depolymerization of polyesters and their packaging formats (e.g., multilayer flexible packaging), but this process can produce significant chemical waste in the form of solvents and excess reagents. Using ball mill grinding (BMG) to overcome the limitations of conventional ester aminolysis, we demonstrate an operationally simple mechanochemical depolymerization of PLA, PHAs, and biodegradable multilayer flexible film packaging. Maintaining a focus on sustainable materials, we then demonstrate the synthesis of tunable α-lipoic acid (αLA)-based resins for photopolymerization to disulfide covalent adaptable networks (CANs) from the depolymerized polyesters in one-pot. Investigation into structure-property relationships reveals a range of mechanical properties— producing significantly softer materials relative to the initial polyester film packaging. Additionally, we demonstrate degradation via disulfide cleavage of the αLA-based materials under conditions that mimic low oxidation-reduction potential (ORP) environments. Ultimately, this work further solidifies the utility of BMG mechanochemistry for mild and sustainable depolymerizations and demonstrates metamorphosis of the depolymerized monomers into bio-based CANs with unique properties while maintaining degradability.

Introduction

Biodegradable polyester materials such as poly(lactic acid) (PLA) and poly(hydroxyalkanoates) (PHAs) are gaining popularity as sustainable alternatives to traditional polyolefins in response to the global plastic waste crisis.[1,2] A lack of widespread and accessible infrastructure to mechanically recycle these plastics has prevented their proper reuse in a circular economy (i.e., recycling/repurposing back to the original material), however.[2,3] While a sustainable end of life for these materials is accessible through composting, this method prevents *repurposing* of the material, demonstrating the need for alternative recycling methods (e.g., chemical recycling).[2] Chemical depolymerization and repolymerization for repurposing polymer waste can give a new life to these plastics (i.e., repurposing of plastic waste into new materials) that incentivizes their recycling via value-added products with newfound properties and built in circularity that differs from the parent feedstock.[4] Polyesters are particularly amenable to depolymerization due to labile ester bonds along the backbone. While hydrolysis and methanolysis maintain the circular PLA economy by producing lactide/lactic acid and methyl lactate, they typically require harsh conditions, catalysts, and large excesses of reagents due to low reaction rates.[5–9] Recently, aminolysis with ethanolamine (EA) has attracted attention as a catalyst-free depolymerization method of aliphatic and aromatic post-consumer polyesters for the formation of amide-containing diols, uniquely poised for later transformations relative to other -lysis products. Using primary amino alcohols (e.g., EA), methods typically result in high yields under relatively mild conditions (e.g., 1 h, 100 ˚C).[9–14] The subsequent diol monomer derived specifically from EA has been used for esterification to a diacrylate for additive manufacturing applications[10] (**Figure 1A**) and polycondensation for the synthesis of poly(ester-amides).[14] While these collective methods are

View Article Online
DOI: 10.1039/D6PY00436A

effective for depolymerization, they still require high temperatures, an inert atmosphere, and/or excess nucleophile, thus limiting their energy efficiency and atom economy. Mechanochemistry via solid-state ball mill grinding (BMG) is uniquely poised to overcome these specific limitations found in traditional solution-state chemistry for polymer degradation and upcycling.[15–17]

Degradation under mechanical force was first described for macromolecular chain scission by Staudinger in the 1930s.[18] Since then, chemists have utilized mechanochemical reactions to depolymerize,[15,19–22] synthesize,[23–26] and functionalize[27,28] a variety of industrially-relevant polymers. In the context of synthetic chemistry, mechanochemistry is lauded for faster kinetics and lower solvent usage relative to solution-state analogs driven by traditional stimuli such as heat and light.[29,30] For polymer science in particular, relevant work showcasing the catalyst- and/or solvent-free mechanochemical hydrolysis of poly(ethylene terephthalate) (PET),[21,22] methanolysis of poly(carbonates) (PC) and PLA,[19] and aminolysis of PC with *tert*-butyl amine[31] have demonstrated BMG to be a sustainable and effective option for depolymerization, forgoing high temperatures and/or catalysts to obtain full substrate conversion (**Figure 1B**). Many of these reported mechanochemical polyester depolymerizations maintain a closed-loop recycling approach, reproducing the initial monomers/material. While closed-loop chemical recycling is useful to recover initial polymer properties without the addition of virgin material, open-loop recycling to a higher value material, such as thermosets/covalent adaptable networks (CANs) with built in circularity, better incentivizes recovery and reuse.[4] Despite widespread efforts on polyester mechanochemical and solution-state depolymerization, methods for subsequent *repolymerization* toward crosslinked materials with dynamic bonds for reprocessability (e.g., disulfide exchange) and inherent circularity/biodegradability remain under explored, especially those from mixed waste systems. In this work, we sought to combine the faster kinetics of aminolysis with the advantages of mechanochemistry to develop a catalyst- and solvent-free aminolysis of aliphatic polyesters with an amino alcohol, focused on PLA, PHAs, and mixed waste film packaging. To further incentivize chemical recycling, we demonstrate emblematic

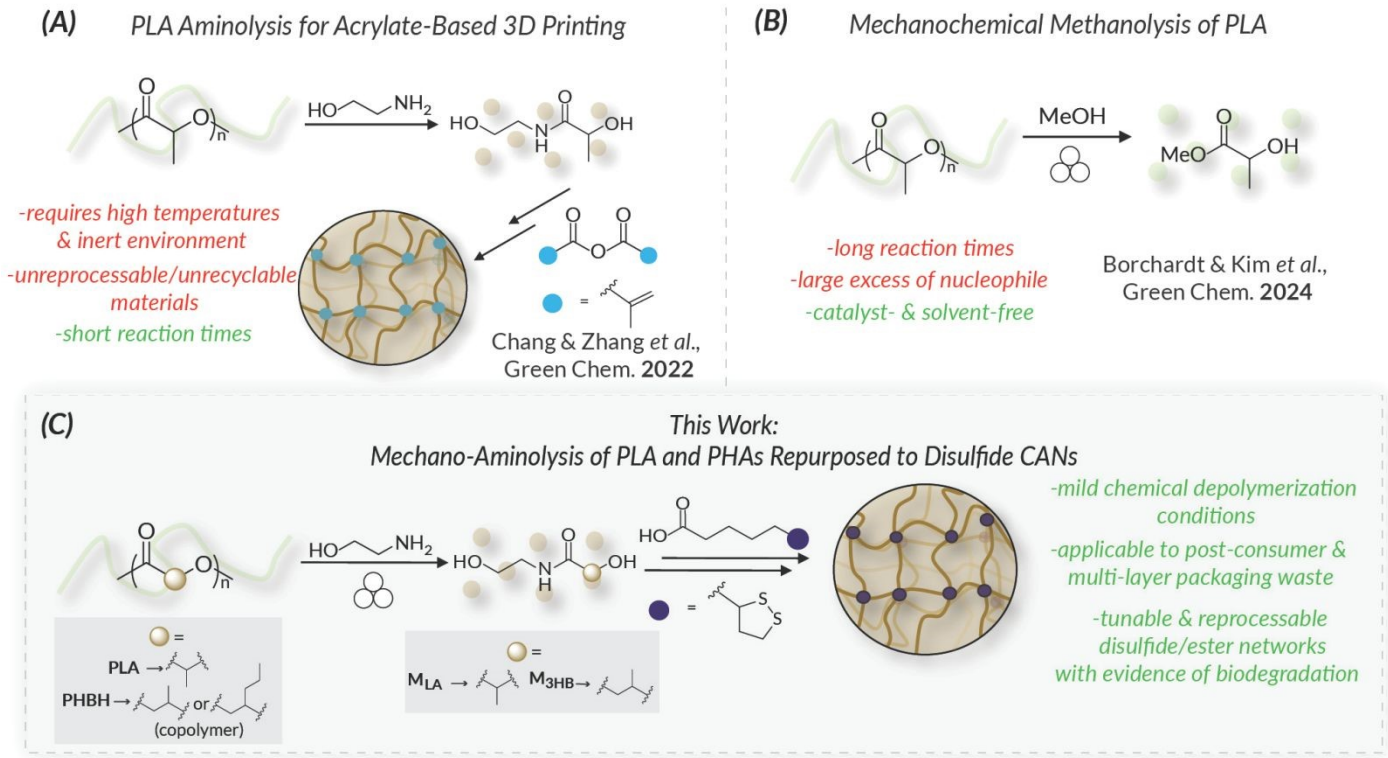

Fig. 1 Inspired by (A) solution-state aminolysis and (B) the state-of-the-art mechanochemical depolymerization of PLA via catalyst-free methanolysis we present (C) this work's mechanochemical aminolysis of PLA and PHAs for covalent adaptable disulfide networks.

View Article Online
DOI: 10.1039/D6PY00436A

repurposing of the resulting diol monomers into one-pot lipoate resins for disulfide CANs from plastic waste with potential as vat photopolymerization resins[32] (**Figure 1C**). Utilizing BMG conditions, we demonstrate improved aminolysis monomer yields of PLA pellets and unprocessed waste (i.e., a PLA cup) relative to solution-state conditions. Notably, our mechanochemical aminolysis method is conducted under air and uses limited excess of nucleophile yet delivers comparable results to previous solvothermal reports. Our catalyst-free depolymerization strategy can also be applied to mixed waste film packaging, a complex material that cannot be mechanically recycled back to polymer, with moderate yields. Steglich-type esterification of the monomers with α-lipoic acid (αLA), a bio-derived disulfide source, and subsequent photopolymerization result in tunable, soft CANs with Young's moduli spanning almost an order of magnitude. These dynamic materials provide a wide range of thermal and mechanical properties that are significantly different than the initial post-consumer material, while maintaining degradability as shown by reductive switching. Overall, we present an operationally simple mechano-aminolysis method for the metamorphosis of plastic waste into bio-derived, degradable CANs.

Results & Discussion

Mechanochemical aminolysis of low molar mass poly(lactic acid)

We first evaluated mechanochemical aminolysis conditions on low molar mass (M_n = 10.8 kDa) semi-crystalline PLLA to test reaction parameters. Building upon previously reported mechanochemical depolymerization conditions for PLA,[19] we elected to utilize a 25 mL stainless steel jar with 50 x 5 mm stainless steel milling balls as a starting point for reaction optimization. Experimentally, PLLA and EA in various ratios were added under air and milled. Force-free PLA aminolysis is typically set up under inert conditions due to high temperatures and long reaction times oxidizing the amine nucleophile. Notably, the use of mechanochemistry to reduce reaction time and temperature enabled us to conduct these reactions under air. Within 0.5 hours and only a slight excess of nucleophile (2.0 equivalents), 80% of the desired diol monomer (M_{LA}) was achieved (**Table 1**), while lower equivalents of EA resulted in lower yields. It was previously reported that under dry milling conditions, rates of mechanochemical chain scission were found to be consistent between both semi-crystalline and amorphous PLA.[33] These similar rates were due to amorphization of the semi-crystalline PLA in under one minute of milling. To determine the effect of PLA's crystallinity on chemical depolymerization efficiency, we synthesized low M_n (21.3 kDa) amorphous PLDLA and subjected it to the optimized reaction conditions. Aminolysis of PLDLA yielded 84% M_{LA}, consistent with previous findings that initial crystallinity did not significantly impact results. To further increase monomer yield, we identified potassium carbonate (K_2CO_3) as a potential additive to activate the polyester backbone, improving electrophilicity even without full solubility.[34] Interestingly, we observed a *decrease* of ca. 30% in M_{LA} production, presumably due to less productive mechanochemical energy transfer due to added volume from the solid base. Notably, the M_{LA} monomer, which we used for structural confirmation and materials screening (*vide infra*), is available commercially at a cost of 1,084 USD per mole. With our depolymerization protocol, the total cost of reagents (PLA_{cup} and ethanolamine) is under 6 USD per mole (**Table S1**).

View Article Online
DOI: 10.1039/D6PY00436A

Table 1: Optimization of mechanochemical aminolysis of low molar mass PLA[a]

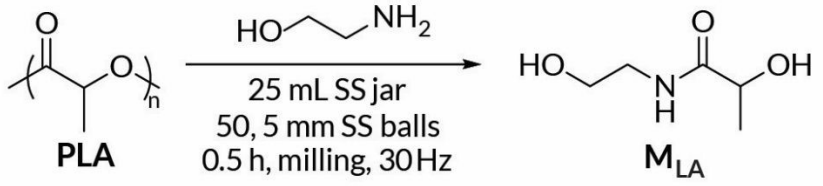

Sample	M_n (kDa)[b]	$Đ$[b]	Ethanolamine (Equiv.)	K_2CO_3 (Equiv.)	Monomer (M_{LA}) Yield (%)[c]
PLLA	10.8	1.2	1.0	0	66
PLLA	10.8	1.2	1.5	0	75
PLLA	10.8	1.2	2.0	0	80
PLDLA	21.3	1.2	2.0	0	84
PLLA	10.8	1.2	2.0	0.5	50

[a]Reaction conditions: PLA repeat unit = 1 mmol. [b]M_n and $Đ$ were determined by GPC-MALS-RI in $CHCl_3$. [c]Monomer yield was determined by ^{1}H NMR spectroscopy using dibromomethane as an internal standard.

Depolymerization of commercial and post-consumer polyester substrates

With optimized depolymerization results from model PLA substrates in hand, we turned our attention to commercial and post-consumer substrates of both PLA and a common PHA copolymer, poly(3-hydroxybutyrate-co-3-hydroxyhexanoate) (PHBH) with approximately 94 mol% 3-hydroxybutyrate (3HB) and 6 mol% of the 3-hydroxyhexanoate (3HH) unit (**Table 2**). For these commercially relevant samples, we initially found that increasing reaction times from 0.5 h to 1 h slightly improved yield, from 76% to 86% M_{LA}, for the 76.4 kDa PLA_{powder} sample (**Table S2** for results of extended reaction times). Additionally, an 89.3 kDa post-consumer PLA cup (PLA_{cup}) was also easily depolymerized with a yield of 77%. We were also interested in the kinetics of the BMG depolymerization, as it appeared to be faster than previous mechanochemical PLA depolymerizations, which took up to 5 h under methanolysis conditions.[19] At short reaction times we observe a yield of 18% in 30 seconds (**Table S2**). We then see the yield continue to increase reaching 65% in 5 minutes, after which the reaction appears to slow until reaching a maximum yield of 86% in 1 hour. While our yields increase linearly under 15 mins, they eventually plateau after 1 h. We hypothesize this is due to the temperature dependent viscoelastic behavior of our polymer substrates during milling and monomer generation over time.[22,35,36] Friction generated from milling increases the bulk jar temperature to 41 ˚C in 0.5 h (**Table S3**). At this temperature, we are approaching the T_g of the PLA_{powder} (56 ˚C), at which increased mobility of the chains can limit effective force collisions by reducing localized stress.[17,35] We also expect effective applied force to decrease as the amount of viscous liquid monomer is generated. This will trap milling media preventing collisions and ultimately generating less friction, which is evidenced by decreasing temperature over long reaction times (**Table S3**). Applying the optimized conditions to a 94.1 kDa PLA pellet (PLA_{pellet}) showed a lower yield of 31% compared to the model PLA yields (ca. 80% product). We found that the PLA_{pellet} was almost 14 times thicker than the PLA_{cup} substrate (**Figure S4**), demonstrating the impact initial bulk morphology and available surface area has on depolymerization efficiency.

Based on our results from the kinetic data and the low yields from the PLA_{pellet} depolymerization, we surmise that mechanochemical aminolysis is occurring on the surface of substrate in a reactive phase. This reactive microenvironment is governed by penetration of the nucleophile into the surface from applied mechanical force.[22,37] Interestingly, the rate of depolymerization is critical at short times to achieve effective

View Article Online
DOI: 10.1039/D6PY00436A

depolymerization. At longer times we observe the yield plateau, likely due to increasing temperature resulting in elastic collisions and generation of monomer that eventually traps milling media, thus inhibiting the reaction phase. Similar mechanisms have previously been described in the mechanochemical depolymerization of other polyesters, such as PET[22,36–38] and PCs.[19,39]

We then evaluated PHBH samples, with the assumption that they would depolymerize similarly to PLA given their comparable repeat unit structures and generally similar mechanical properties. Despite reaction times up to 3 h and the addition of a 0.5 h cryogenic temperature (ca. –196 ˚C) pre-milling step, we saw a significant decrease in yield compared to PLA. Yields of 20% and 25% of the expected monomer, M_{3HB}, were obtained from both the $PHBH_{pellet}$ (200 kDa) and $PHBH_{powder}$ (148 kDa), respectively. We also noted the presence of alkene resonances at 5.95 and 6.77 ppm in our ^{1}H NMR spectra from these depolymerizations (**Figure S12**). These resonances can be attributed to the formation of crotonic and isocrotonic acid derivatives from a competing E1cB reaction, which has been previously observed in solution-state aminolysis of PHB.[40] Although this competing reaction resulted in a slight decrease in yield, it does not explain the significant difference in reactivity between PHBH and PLA. We hypothesized that unlike PLLA, PHBH fails to fully amorphize under mechanical stress. After pre-milling and during aminolysis, the bulk temperature of the jar increases, so that milling occurs well above PHBH's glass transition temperature (T_g = –4 ˚C). At the bulk jar temperature of ca. 42 ˚C, PHBH exists in the rubbery region, resulting in more elastic collisions between the polymer and the milling media and subsequently limiting the depth at which the nucleophile can penetrate the polymer particle under mechanical force. Although measured at room temperature, this is exemplified by the differences in stiffness of the materials. The commercial PLA substrate is roughly 3 times stiffer than PHBH and has a significantly higher T_g (**Table S6**), rendering PLA's degradation under the same mechanical force faster before the effective applied force is limited from increasing elastic deformations and trapped milling media. It is also likely that the effective applied force generated during milling does not provide sufficient transfer of kinetic energy to break crystallites in a low T_g material. Retention of crystallinity could explain lower depolymerization yields, as crystallinity can correlate to chemical resistivity.[41] Semi-crystalline structure in PHBH was confirmed by presence of melting peaks via differential scanning calorimetry (DSC) (**Figure S44**). After milling the polymer for 0.5 h at room temperature, apparent crystallinity only decreased by ca. 5% (**Figure S45**). Milling at cryogenic temperatures also had little impact on apparent crystallinity (**Figure S46** and **S47**); however, we found that introducing a cryogenic temperature pre-milling procedure prior to $PHBH_{powder}$ depolymerization minimally increased yields from 18% to 25%, presumably due to decreased molar mass after pre-milling (**Table S4** and **Figure S8**). To further confirm crystallinity impacts PHBH depolymerization yields, we also evaluated an amorphous PHA (aPHA) of a similar molar mass as the other substrates (ca. 180 kDa). aPHA is a copolymer of ca. 60 mol% 3-hydroxybutyrate and 40 mol% 4-hydroxybutyrate, resulting in both M_{3HB} and M_{4HB} products from depolymerization, respectively. Under the standard 3 h reaction conditions (no pre-milling), both aPHA bulk morphologies (i.e., 183 kDa $aPHA_{powder}$ and 174 kDa $aPHA_{pellet}$) show a significant increase in total monomer yield (M_{3HB} and M_{4HB}) compared to PHBH, from 25% to 43% for the $PHBH_{powder}$ and $aPHA_{powder}$, respectively. We do also observe formation of elimination byproducts from the aminolysis of aPHA as well (**Figure S14**). The increase in yield for less crystalline PHA substrates supports our hypothesis that amorphization is critical to the initial mechanochemical depolymerization of aliphatic polyesters in our BMG system. If crystallinity were the only factor determining sufficient depolymerization, however, we would have expected the yield of $aPHA_{powder}$ to match that of the PLA_{powder}. Therefore, we note that the thermomechanical behavior (i.e., T_g and viscoelasticity at reaction temperature) of the polymer also likely plays a role in the efficiency of depolymerization. As aPHA has a T_g of –20 ˚C, we expect that like PHBH, aPHA is being milled in the rubbery region and dissipating energy at short reaction times to prevent more efficient depolymerization.

View Article Online
DOI: 10.1039/D6PY00436A

To demonstrate the utility of BMG compared to thermal stimuli, we conducted force-free stirred controls at 42 ˚C (**Figure S5** and **Table S5**), the highest temperature recorded on the surface of the milling jars (see **Table S3** for surface temperatures over extended milling times) under an inert N_2 atmosphere. Most notably, yields from the mechanochemical aminolysis of the PLA_{cup} and the PLA_{pellet} were significantly higher than their force-free counterparts— <5% monomer yield for both substrates without applied force and up to 77% for the PLA_{cup} under mechanochemical conditions. This significant increase in yield for the PLA_{cup} is likely due to the reduction in particle sizes during ball milling to increase surface area, relative to the pellet substrates that are still more challenging to mechanochemically depolymerize than the other morphologies likely due to their thickness/lower surface area. When milling the pellets near/above PLA_{pellet}'s and $PHBH_{pellet}$'s T_gs, we observe less effective comminution, as evidenced by our recovery of smaller pellets after depolymerization. Unreacted pellets were also retrieved at extended reaction times, with no improvement in yield. However, we do observe higher monomer yields overall for the depolymerization of unprocessed substrates. Improved monomer yields under mild conditions demonstrates the inherent value of mechanochemistry over traditional solution-state processes. It should be noted that because these BMG reactions are run in stainless steel containers, we cannot entirely rule out iron catalysis from the jar/milling ball surfaces.[19,42]

Table 2: Mechanochemical aminolysis of various polyester substrates[a]

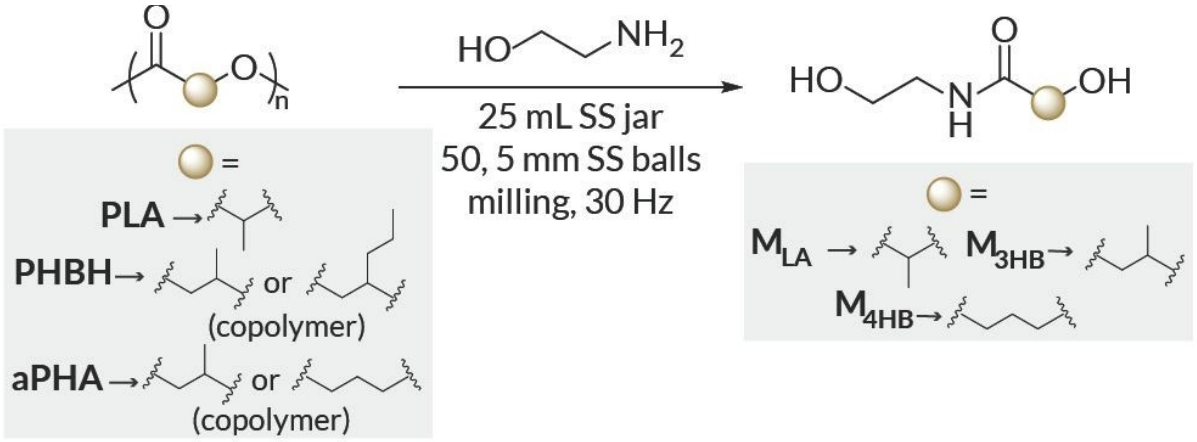

Sample	M_n (kDa)[b]	$Đ$[b]	Reaction Time (h)	Total Monomer Yield (%)[c]
PLA_{pellet}	94.1	1.3	1	31
PLA_{powder}	76.4	1.4	1	86
PLA_{cup}	89.3	1.3	1	77
$PHBH_{pellet}$[d]	200	2.2	3	20[e]
$PHBH_{powder}$[d]	148	1.8	3	25[e]
$aPHA_{pellet}$	174	1.5	3	40[f]
$aPHA_{powder}$	183	1.4	3	43[f]

[a]Reaction conditions: polymer repeat unit = 1 mmol and EA = 2 mmol. [b]M_n and $Đ$ were determined by GPC-MALS-RI in $CHCl_3$. [c] Total monomer yield was determined by ^{1}H NMR spectroscopy using dibromomethane as an internal standard. [d]Substrates were pre-milled for 0.5 h at cryogenic temperatures before aminolysis (See SI for details). [e] Total monomer yield refers to the product from the 3-hydroxybutyrate unit only (M_{3HB}). The 3-hydroxyhexanoate (3HH) product was not observed spectroscopically (See SI for details). [f] Total monomer yield refers to both M_{3HB} and M_{4HB}.

View Article Online
DOI: 10.1039/D6PY00436A

Synthesis, photopolymerization, and characterization of lipoate materials

Inspired by recent developments in sustainable disulfide CANs,[43,44] we selected naturally sourced α-lipoic acid (αLA) as an emblematic example for the synthesis of thermosets from our resultant monomers. Poly(lipoate)s and their networks have gained significant popularity in recent years as photopolymerizable materials,[44–51] adhesives,[52–55] and copolymer resins.[56,57] The 1,2-dithiolane moiety of αLA is unique in that it enables photopolymerization, reprocessability, and degradation back to monomer via an assortment of chemical or thermal methods (**Figure 2A**).[58] In addition to self-healing properties via dynamic backbone exchange, disulfides can also undergo reductive exchange with small molecule thiols, opening up additional degradation pathways. For example, when disulfides are engineered into the aliphatic polyester poly(butylene succinate), they enable an additional biodegradation pathway via reductive switching; these results suggest potential degradation mechanisms in marine sediment environments for other disulfide materials.[59] In addition to the dynamic benefits of disulfide bonds, formation of lipoates from αLA via esterification improves thermal stability and also reintroduces labile ester groups for further depolymerization methods and potential biodegradation, as evidenced by incorporation of low molar mass (ca. 3 kDa) to commercial, telechelic PLA-OH into compostable disulfide CANs (**Figure 2B**).[44] While this example provides evidence for the biodegradation of lipoate photopolymers, this material cannot utilize post-consumer PLA which has unknown chain-ends and high molar masses. The PLA-OH lipoate material is also limited in its tunability, providing access only to bislipoates and subsequently only stiff networks. We therefore envisioned our diol monomers as a basis for soft and tunable circular-by-design thermosets with potential applications in sustainable additive manufacturing from plastic waste.[32] Our depolymerization and repurposing workflow thus adds an orthogonal end of life to aliphatic polyesters as new CANs while maintaining access to a library of chemical depolymerization, reprocessing, and degradation strategies due to their disulfide (i.e., thiol exchange) [60] and ester bonds (i.e., environmental hydrolysis or microbial degradation in the environment).[61,62]

After the successful depolymerization of various polyesters, we turned our attention to repurposing the diol monomers (M_{LA} from PLA and M_{3HB} from PHBH) into αLA-based resins for photopolymerization inspired by lipoate materials from Worch and Dove[43,63] and Hawker, Choi, Read de Alaniz, and Bates,[45,46,48] among many others.[33,36,42,50] For ease of materials screening, we used commercially sourced M_{LA} (see **Table S1** for cost comparison) to synthesize resins consisting of both lipoate monomer ($M_{LA}Lp_1$, a mixture of mono-substitution of the primary alcohol $M_{LA}Lp_{1\text{-}1}$ and the secondary alcohol $M_{LA}Lp_{1\text{-}2}$) and dimer ($M_{LA}Lp_2$) via one-pot Steglich esterification with αLA. Different monomer to dimer ratios were obtained by tuning the stoichiometry of αLA to M_{LA} in the esterifications (**Figure 3A**). Notably, previous methods of lipoate resin syntheses do not produce resins with tunable amounts of crosslinker that are directly photopolymerizable, thereby allowing us to omit other monomers/diluents necessary in other formulations. Additionally, some lipoate dimers can show a lack of stability and require the aforementioned monomer/diluent to prevent gelation, thereby making synthesis and isolation challenging.[43]

After esterification, the resins (as a mixture of monomer and dimer) are readily polymerized under 405 nm light upon the addition of 1 mol% diphenyl(2,4,6-trimethylbenzoyl)phosphine oxide (TPO) as a photointiator. To understand the curing behavior of the disulfide resins, we conducted photorheology experiments at 405 nm, a shear gap of 300 μm and an intensity of 20 mW cm^{-2}. The photorheology experiments showed crossover of the storage modulus and loss modulus (i.e., gel point) in 21–38 s for the M_{PLA} resins, which show promise for 3D printing applications at higher intensities (40 mW cm^{-2}) and smaller layers (ca. 5 μm) (**Table S6** and **Figures S65–S69**). We first evaluated several materials derived from M_{LA} resins to understand the material properties as a function of crosslinker loading. To validate the network structure, we estimated crosslink density (ν_e) using classical rubber elasticity theory (i.e., $\nu_e = 3E'/RT$, **Table S8**).[65] We found that that ν_e increases as the mol% of

View Article Online
DOI: 10.1039/D6PY00436A

dimer increases, 20 mol% dimer gave a crosslink density of 93 mol/m^3 while 60 mol% dimer gave 911 mol/m^3.We also determined gel fractions for the materials; all M_{LA} formulations gave gel fractions of 94% or higher. DSC analysis of a sample from each M_{LA} lipoate CAN formulation revealed that higher crosslinker loading positively correlated with glass transition temperature (T_g = –21 to –1 ˚C) (**Figure 3B**). Uniaxial tensile testing showed a similar correlation, resulting in a range of mechanical properties for the soft M_{LA} networks (**Figure 3C**). The lowest crosslinker loading, 20 mol%, showed a Young's modulus of 1.10 ± 0.06 MPa and ultimate tensile strength (UTS) of 0.39 ± 0.02 MPa, while a higher crosslinker loading of 60 mol% resulted in a Young's modulus of 8.73 ± 0.01 MPa and UTS of 2.18 ± 0.24 MPa. Dynamic mechanical analysis (DMA) also confirmed that these materials exhibit dynamic behavior at elevated temperatures (**Figure 3D**). Due to the presence of sufficient disulfide bonds, stress relaxation experiments at 130 ˚C showed relaxation time, τ*, increased with greater amounts of crosslinker. Stress relaxation experiments of a single network at various temperatures also exhibited Arrhenius behavior, typical of other disulfide CANs, resulting in an activation energy (E_a) of 121.6 kJ/mol (**Figure S6**).[47] While our materials also contain free hydroxyl groups, it is unlikely that transesterification contributes to operative bond exchange without an appropriate catalyst. While there are no reports of uncatalyzed transesterification in dual dynamic disulfide/ester networks,[66] hyperbranched epoxy vitrimers have been reported to undergo catalyst-free transesterification.[67] Although excess free hydroxyls can lower the E_a for stress

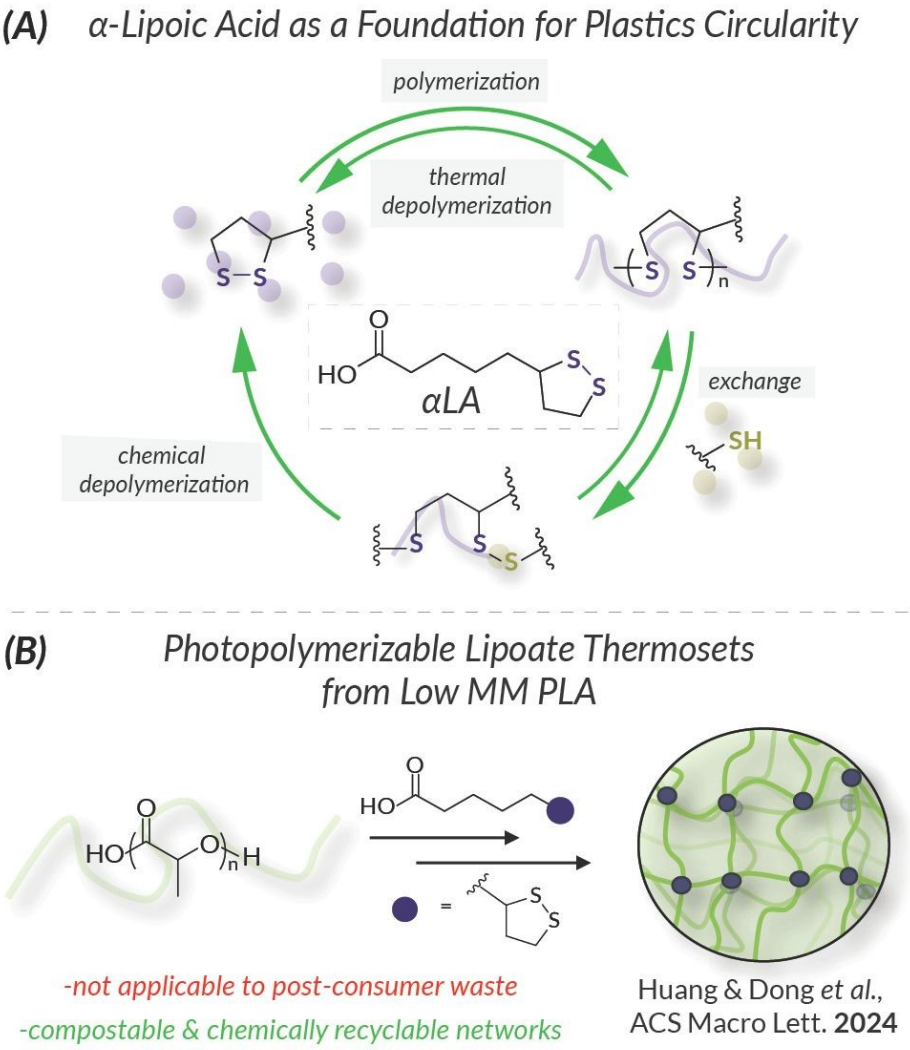

Fig. 2 (A) α-lipoic acid in thermoplastics and thermosets enables a circular plastics economy via thermal depolymerization, exchange with small molecule thiols, and chemical depolymerization in addition to (B) remaining biodegradable and chemically recyclable in disulfide/ester CANs.

View Article Online
DOI: 10.1039/D6PY00436A

relaxation, the hyperbranched structure was also found to play a crucial role in faster stress relaxation, therefore we estimate the impact of transesterification at high temperature is minimal. Importantly, when we implemented a combined mechanochemical PLA depolymerization and repurposing workflow (i.e., lipoate synthesis and photopolymerization with M_{LA} sourced from our mechanochemical PLA depolymerizations), disulfide CAN properties of the depolymerized/repurposed PLA (rPLA) were consistent with those of commercially sourced M_{LA}-based materials (**Table S7**) and gave comparable estimated crosslink densities and gel fractions (**Table S8**). We also evaluated lipoate network formation from a synthesized M_{3HB} to investigate how backbone structure could impact material properties relative to M_{LA}-based CANs. The 89:11 mol% $M_{3HB}Lp_1$:$M_{3HB}Lp_2$ material demonstrated a lower T_g of –37 ˚C, a significantly lower stiffness (0.20 ± 0.02 MPa), and a much higher elongation at break of 88% relative to ca. 40% when compared to the M_{LA} photopolymers, as expected with a lower crosslinker loading and longer aliphatic chain. All networks are thermally stable up to ca. 200 ˚C as shown by thermogravimetric analysis (**Figure S37**). With the addition of the M_{3HB} lipoate network, we were able to access soft materials with a range of Young's moduli that span almost an order of magnitude (**Table S6**). As compared to commercial PLA and PHBH, the photocured lipoate materials are significantly softer, maintain reprocessability (as demonstrated by their ability to stress relax), and can be chemically recyclable due to the preservation of ester bonds. These materials are also well poised to undergo additional chemical recycling strategies via disulfide exchange.[61,66] Although this small selection of photopolymers exhibit a limited scope of mechanical properties, our soft/flexible CANs with greater amounts of crosslinker (e.g., 40 mol% and 60 mol%) do exhibit comparable UTS and elongation at break to some commercial additive manufacturing resins (**Table S9**) and previously reported αLA 3D printed materials.[43] We therefore envision these materials serving as potential (bio)degradable and self-healable resins for the additive manufacturing of flexible parts. Notably, our materials expand upon previous lipoate materials to make use of cheap and abundant plastic waste feedstocks, thereby incorporating sustainability via circular-by-design materials.

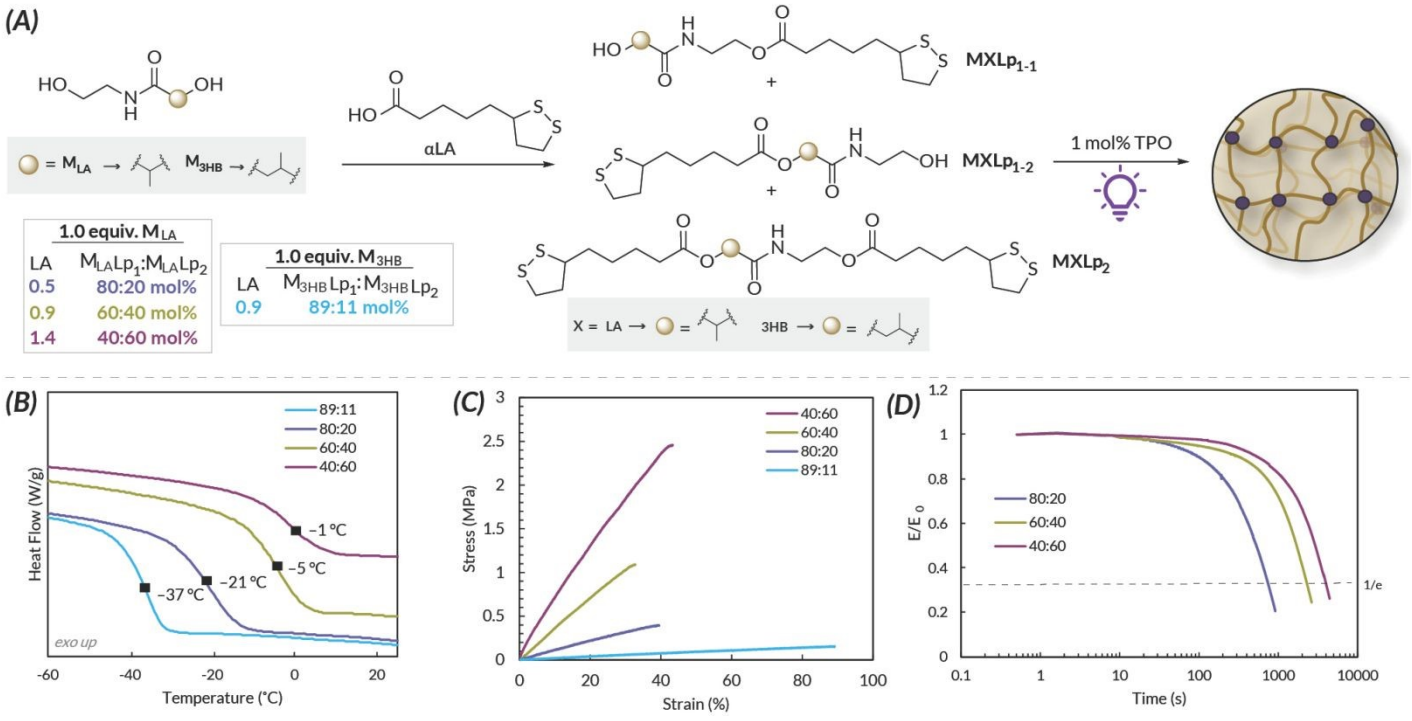

Fig. 3 (A) Reaction scheme depicting the synthesis and photopolymerization of lipoic acid-based disulfide resins. (B) DSC curves, (C) representative stress vs. strain experiments from uniaxial tensile tests (5 mm/min strain rate), and (D) stress relaxation experiments conducted at 130 ˚C of several M_{LA}-lipoate formulations.

View Article Online
DOI: 10.1039/D6PY00436A

Mechanochemical aminolysis and repurposing of polyester multilayer film packaging

To ultimately demonstrate broad applicability of this process to complex polyester post-consumer waste, we selected a multilayer laminated flexible film packaging (FP) substrate containing both PLA and PHBH (ca. 84 wt% polymers), along with significant amounts of proprietary additives/dyes (ca. 16 wt%), to showcase our mechanochemical aminolysis workflow. Notably, multilayer film packaging can be too complex for effective mechanical recycling and physical separation methods (i.e., solvent-targeted recovery and precipitation) require large amounts of solvent to separate individual polymers and can be considered cost-prohibitive.[68] Therefore, we envision our mechanochemical process to quickly break apart the FP substrate for depolymerization and enable subsequent separation of small molecule products from residual film material. Based on estimated amounts of each polymer in the film (See SI for details), we obtain ca. 45% combined yield of M_{LA} and M_{3HB} (**Figure 4A**). We hypothesize that a lower yield results from the FP additives that "cushion" force impacts, as seen in other mechanochemical reactions.[69] Both structures were confirmed by NMR spectroscopy and mass spectrometry of depolymerization reaction (**Figures S13**, **S23**, and **S31**). Scaling the reaction from 150 mg FP to 390 mg (65 mL reaction jar, 32 x 10 mm milling balls, at 17.7 Hz) afforded similar results (39% yield) when milled under an inert environment (N_2) (**Figure 4B**). After esterification, the depolymerized film was repurposed to a lipoate resin with a formulation of 50:50 mol% M_XLp_1:M_XLp_2 (rFP), where x is LA *and* 3HB. Most notably, this formulation contained lipoate monomer and dimer based upon *both* depolymerized PLA and PHBH to access a cured thermosetting material with distinct properties from those of the individual materials alone (**Figure 4C**). Despite a crosslinker loading of 50 mol%, after photopolymerization the rFP CAN shows a lower T_g of –39 ˚C relative to the other $M_{LA}Lp_1$:$M_{LA}Lp_2$ materials (**Table S6**). We found that rFP has a ν_e of 202 mol/m^3 and a gel fraction of 99% (**Table S8**). The rFP lipoate network maintains mechanical properties most comparable to that of 60:40 mol% $M_{LA}Lp_1$:$M_{LA}Lp_2$, as assessed by uniaxial tensile tests. Between the rFP and the 60:40 mol% $M_{LA}Lp_1$:$M_{LA}Lp_2$ materials, there is little difference in extensibility, with both breaking at ca. 35% strain. The rFP is also less stiff (Young's modulus of 2.40 ± 0.03 vs. MPa 3.39 ± 0.01 MPa) with a slightly lower UTS (0.82 ± 0.04 MPa vs. 1.08 ± 0.03 MPa) than the 60:40 formulation. The initial FP material has markedly different mechanical properties to its repurposed counterpart (**Figure 4C**). The rFP CAN also shows the ability to stress relax, with $\tau^* = 670$ s at 130 ˚C (**Figure S63**), suggesting this material can be reprocessed at high temperatures, unlike the FP substrate which is challenging to mechanically recycle. Tensile tests show the FP has an elastic modulus of 161 ± 19 MPa and UTS of 52 ± 10 MPa, which are both ca. 50 times higher than that of the rFP CAN; thus, demonstrating the metamorphosis of a stiff thermoplastic material to a soft and dynamic disulfide CAN with a reinstalled polyester backbone for multiple potential degradation routes, such as disulfide reduction.

Degradation of lipoate networks

Alongside many previous examples demonstrating the chemical and/or thermal depolymerization of lipoate photopolymers, we conducted reductive degradation of the 80:20 mol% $M_{LA}Lp_1$:$M_{LA}Lp_2$ film (**Figure 5A** and **Table S9**) using a small molecule dithiol, D,L-dithiothreitol (DTT), which mimics low oxidation-reduction potential (ORP) environments (i.e., marine sediment)[59,70] to induce thiol exchange for de-crosslinking (**Figure 5B**). After stirring in a 0.1 M solution of DTT in phosphate buffer solution (PBS) for six days, the lipoate network is largely degraded to water soluble products, with only 39% mass remaining compared to >100% mass remaining for our lipoate material in PBS only. The PLA/PHBH based film packaging material (FP) was also subjected to reaction conditions as a negative control, as the ester linkages should not undergo significant depolymerization with DTT. Under the reductive conditions, FP returned 96% of its initial mass after six days, suggesting our lipoate material could undergo much faster degradation than the FP material in low ORP marine sediment-like environments due to the presence of disulfide bonds in the CANs.

View Article Online
DOI: 10.1039/D6PY00436A

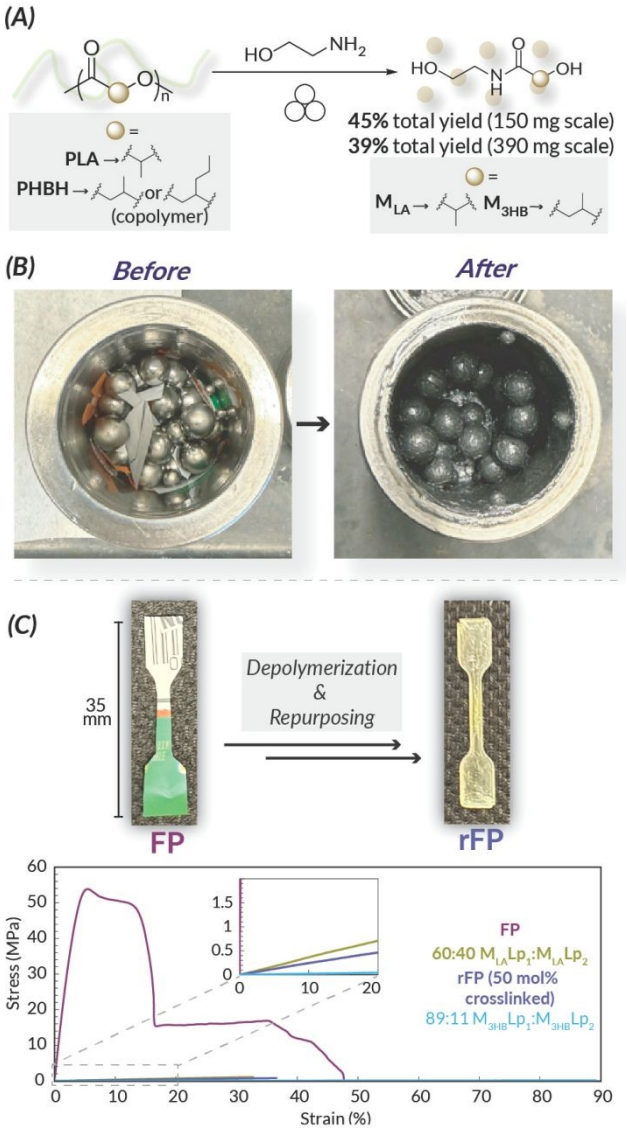

Fig. 4 (A) Reaction scheme demonstrating the depolymerization of a mixed polyester multilayer flexible packaging (FP) containing both PLA and PHBH with (B) images showing the 65 mL ball mill jars before and after the 390 mg scale depolymerization of the FP substrate. (C) Representative stress vs. strain experiments from uniaxial tensile tests comparing the mixed polyester film packaging (FP, image left) with the lipoate CANs from the repurposed FP (rFP, 50 mol% crosslinked, image right) and 60:40 mol% $M_{LA}Lp_1$:$M_{LA}Lp_2$ and 89:11 mol% $M_{3HB}Lp_1$:$M_{3HB}Lp_2$ materials.

Conclusions

Ball mill grinding mechanochemistry allows for the mild (i.e., room temperature) and fast depolymerization of polyesters, such as PLA, with no catalyst or solvent and limited excess reagents in yields up to 87% of a diol monomer. PHBH was found to be more difficult to depolymerize due to retention of crystallinity and viscoelastic properties under ball milling conditions, as evidenced by an improved monomer yield of 43% for an amorphous PHA substrate. Additionally, we observed a competing elimination reaction under mechanochemical aminolysis conditions for both PHAs. Ball mill grinding mechanochemistry specifically improved depolymerization yields compared to those in solution of post-consumer substrates (e.g., PLA cup) by inducing reaction on the surface of polymer particles, as evidence by kinetic data at short reaction times and

View Article Online
DOI: 10.1039/D6PY00436A

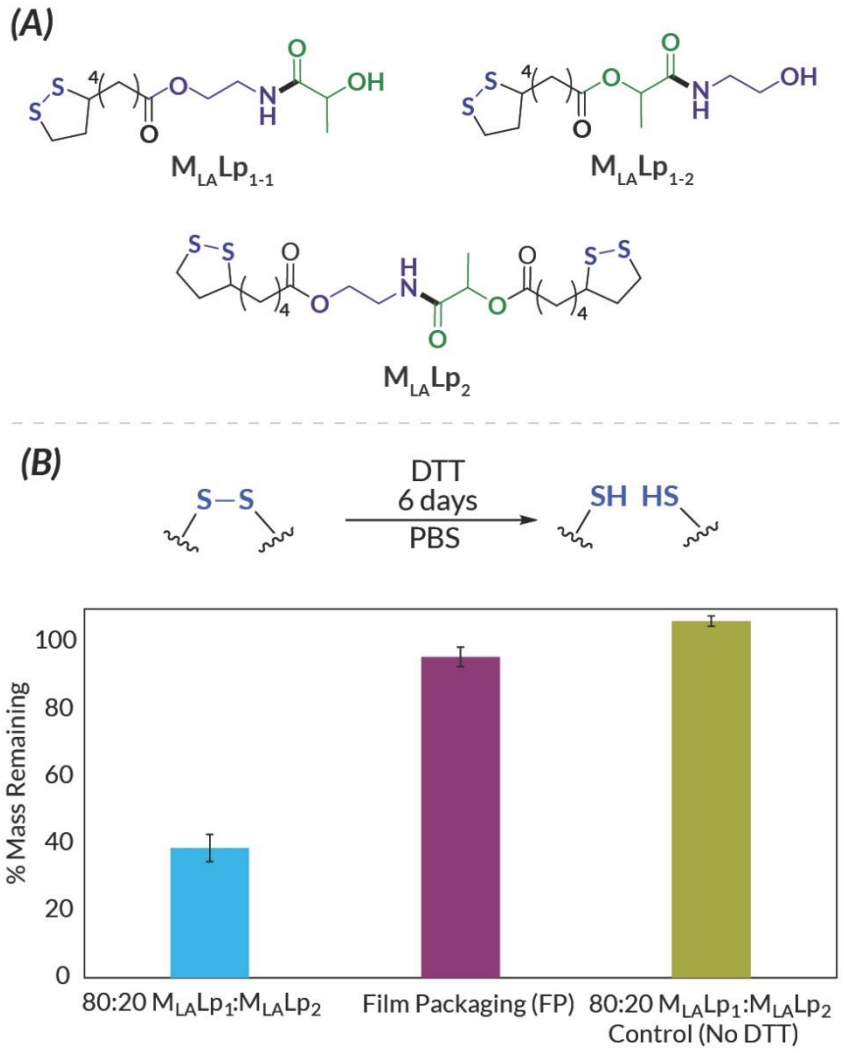

Fig. 5 (A) Monomer and crosslinker structures in the lipoate CAN. (B) Reaction scheme depicting reduction of the CAN's disulfide bonds and crosslinks (top) and a bar graph (bottom) showing the percent mass remaining of the 80:20 M_{LA}-based network and the FP substrate which contains no disulfide bonds after stirring with DTT, and the 80:20 M_{LA}-based CAN after stirring in only PBS for 6 days.

recovery of PLA substrates with higher surface areas. Using an esterification with α-lipoic acid, we accessed a range of tunable disulfide CANs with low elastic moduli (0.20–8.73 MPa) and moderate elongation from M_{LA} or M_{3HB} comparable to some previous lipoate materials and commercial flexible additive manufacturing resins. Our mechano-aminolysis and repurposing framework can also be applied to a multilayer laminated film packaging (FP) consisting of both PLA and PHBH. Lipoate materials from the FP substrate (rFP) resulted in a Young's modulus of 2.40 MPa, UTS of 0.82 MPa, and elongation of 39%, supplying a significantly softer and dynamic material capable of reprocessing and multiple routes for chemical recycling as compared to the initial film packaging. As an orthogonal method to chemical recycling, we demonstrated reductive degradation of the lipoate networks in a low ORP environment, mimicking marine sediment. Under these conditions, a representative M_{LA}-based network lost 61% of its initial mass after only six days. We anticipate future scalability of force-driven depolymerization to focus on mechanochemical tools already present in industry. Utilization of thermomechanical processing (i.e., twin-screw extrusion)[71,72] and/or larger milling equipment (i.e., planetary or drum mills),[17] as guided by proof-of-concept lab scale BMG[15] and several recent kinematic models for mechanochemical reactions,[73–76] present promising routes for the incorporation of mechanochemical depolymerization at scale. We

View Article Online
DOI: 10.1039/D6PY00436A

also envision future application of mechanochemical aminolysis to other commercial relevant polyesters, such as PET, which should be reactive under these mechanochemical conditions. Overall, these findings demonstrate the broad utility of lab-scale ball mill grinding for operationally simple and sustainable depolymerizations of complex polymer waste for repurposing to dynamic and degradable α-lipoic acid-derived soft networks.

Associated Content

Supporting Information: Experimental and synthetic procedures, analytical spectra (NMR, MS), chromatograms (GPC), and materials characterization (DSC, TGA, DMA, tensile testing, photorheology).

Author Information

Corresponding Author: goldermr@uw.edu

Author Contributions

M.E.S. and M.R.G. conceived of the idea. M.E.S, Q.Y., and K.A.P. conducted synthetic experiments. M.E.S. synthesized and characterized networks. A.P.K.V. conducted photorheology experiments. M.E.S. and M.R.G. wrote the manuscript; all authors discussed and edited the manuscript.

Conflicts of Interest

S. N-S. is employed by PepsiCo. All other authors have no conflicts to declare. The views expressed in this manuscript are those of the authors and do not necessarily reflect the position or policy of PepsiCo, Inc.

Acknowledgements

This work was supported by generous start-up funds from the University of Washington and support from PepsiCo. M.E.S. acknowledges the University of Washington Clean Energy Institute for a graduate research and Ph.D. completion fellowship. DSC and DMA instrumentation is funded by the Student Technology Fund (STF) at the University of Washington. The authors thank Prof. Dianne Xiao for use of TGA instrumentation, Prof. Alshakim Nelson for use of a load frame, Dr. Martin Sadilek and Brandon Bol for assistance with MS, DSC, and DMA, Brian Sun for assistance with DMA, and Dr. Naroa Sadaba for assistance with the load frame. The authors thank Prof. Chen Wang and his students (University of Utah) for helpful discussions. This material is based in part upon work supported by the state of Washington through the University of Washington Clean Energy Institute. NMR spectroscopy resources are supported under NIH S10 OD030224-01A1.

References

(1) Chen, G.-Q.; Patel, M. K. Plastics Derived from Biological Sources: Present and Future: A Technical and Environmental Review. *Chem. Rev.* **2012**, *112* (4), 2082–2099. https://doi.org/10.1021/cr200162d.
(2) Shi, C.; Quinn, E. C.; Diment, W. T.; Chen, E. Y.-X. Recyclable and (Bio)Degradable Polyesters in a Circular Plastics Economy. *Chem. Rev.* **2024**, *124* (7), 4393–4478. https://doi.org/10.1021/acs.chemrev.3c00848.

View Article Online
DOI: 10.1039/D6PY00436A

(3) Epps, T. H.; Korley, L. T. J.; Yan, T.; Beers, K. L.; Burt, T. M. Sustainability of Synthetic Plastics: Considerations in Materials Life-Cycle Management. *JACS Au* **2022**, *2* (1), 3–11. https://doi.org/10.1021/jacsau.1c00191.
(4) Jehanno, C.; Alty, J. W.; Roosen, M.; De Meester, S.; Dove, A. P.; Chen, E. Y.-X.; Leibfarth, F. A.; Sardon, H. Critical Advances and Future Opportunities in Upcycling Commodity Polymers. *Nature* **2022**, *603* (7903), 803–814. https://doi.org/10.1038/s41586-021-04350-0.
(5) Cederholm, L.; Wohlert, J.; Olsén, P.; Hakkarainen, M.; Odelius, K. "Like Recycles Like": Selective Ring-Closing Depolymerization of Poly(L-Lactic Acid) to L-Lactide. *Angewandte Chemie International Edition* **2022**, *61* (33), e202204531. https://doi.org/10.1002/anie.202204531.
(6) Alberti, C.; Enthaler, S. Depolymerization of End-of-Life Poly(Lactide) to Lactide via Zinc-Catalysis. *ChemistrySelect* **2020**, *5* (46), 14759–14763. https://doi.org/10.1002/slct.202003979.
(7) Spicer, A. J.; Brandolese, A.; Dove, A. P. Selective and Sequential Catalytic Chemical Depolymerization and Upcycling of Mixed Plastics. *ACS Macro Lett.* **2024**, *13* (2), 189–194. https://doi.org/10.1021/acsmacrolett.3c00751.
(8) McGuire, T. M.; Buchard, A.; Williams, C. Chemical Recycling of Commercial Poly(l-Lactic Acid) to l-Lactide Using a High-Performance Sn(II)/Alcohol Catalyst System. *J. Am. Chem. Soc.* **2023**, *145* (36), 19840–19848. https://doi.org/10.1021/jacs.3c05863.
(9) Li, Y.; Wang, S.; Qian, S.; Liu, Z.; Weng, Y.; Zhang, Y. Depolymerization and Re/Upcycling of Biodegradable PLA Plastics. *ACS Omega* **2024**, *9* (12), 13509–13521. https://doi.org/10.1021/acsomega.3c08674.
(10) Shao, L.; Chang, Y.-C.; Hao, C.; Fei, M.; Zhao, B.; Bliss, B. J.; Zhang, J. A Chemical Approach for the Future of PLA Upcycling: From Plastic Wastes to New 3D Printing Materials. *Green Chem.* **2022**, *24* (22), 8716–8724. https://doi.org/10.1039/D2GC01745H.
(11) Fukushima, K.; Lecuyer, J. M.; Wei, D. S.; Horn, H. W.; Jones, G. O.; Al-Megren, H. A.; Alabdulrahman, A. M.; Alsewailem, F. D.; McNeil, M. A.; Rice, J. E.; Hedrick, J. L. Advanced Chemical Recycling of Poly(Ethylene Terephthalate) through Organocatalytic Aminolysis. *Polym. Chem.* **2013**, *4* (5), 1610–1616. https://doi.org/10.1039/C2PY20793A.
(12) Zhou, X.; Chai, M.; Xu, G.; Yang, R.; Sun, H.; Wang, Q. Catalyst-Free Amino-Alcoholysis Depolymerization Strategy: A Facile and Powerful Tool for Chemical Recycling of Poly(Bisphenol A Carbonate). *Green Chem.* **2023**, *25* (3), 952–959. https://doi.org/10.1039/D2GC03568E.
(13) Cheng, K.; Hsu, Y.-I.; Uyama, H. Solvent-Promoted Catalyst-Free Aminolytic Degradation for Chemical Recycling of Single and Mixed Plastic Wastes. *Green Chem.* **2025**, *27* (25), 7620–7630. https://doi.org/10.1039/D5GC01068C.
(14) Liu, S.; Hu, L.; Liu, J.; Zhang, Z.; Suo, H.; Qin, Y. Zinc Catalyst for Chemical Upcycling of PLA Wastes: Novel Industrial Monomer Resource toward Poly(Ester–Amide). *Macromolecules* **2024**, *57* (10), 4662–4669. https://doi.org/10.1021/acs.macromol.4c00360.
(15) Aydonat, S.; Hergesell, A. H.; Seitzinger, C. L.; Lennarz, R.; Chang, G.; Sievers, C.; Meisner, J.; Vollmer, I.; Göstl, R. Leveraging Mechanochemistry for Sustainable Polymer Degradation. *Polym J* **2024**. https://doi.org/10.1038/s41428-023-00863-9.
(16) Briš, A.; Margetić, D.; Štrukil, V. Mechanochemical Ball Milling as an Emerging Tool in Chemical Recycling and Upcycling of Waste Polymers. *Green Chem.* **2025**, *27* (45), 14401–14435. https://doi.org/10.1039/D5GC03507D.
(17) Rizzo, A.; Peterson, G. I. Progress toward Sustainable Polymer Technologies with Ball-Mill Grinding. *Progress in Polymer Science* **2024**, *159*, 101900. https://doi.org/10.1016/j.progpolymsci.2024.101900.
(18) Staudinger, H.; Heuer, W. Über hochpolymere Verbindungen, 93. Mitteil.: Über das Zerreißen der Faden‐Moleküle des Poly‐styrols. *Ber. dtsch. Chem. Ges. A/B* **1934**, *67* (7), 1159–1164. https://doi.org/10.1002/cber.19340670708.
(19) Lee, H. W.; Yoo, K.; Borchardt, L.; Kim, J. G. Chemical Recycling of Polycarbonate and Polyester without Solvent and Catalyst: Mechanochemical Methanolysis. *Green Chem.* **2024**, *26* (4), 2087–2093. https://doi.org/10.1039/D3GC03643J.

View Article Online
DOI: 10.1039/D6PY00436A

(20) Pérez-Venegas, M.; Friščić, T.; Auclair, K. Efficient Mechano-Enzymatic Hydrolysis of Polylactic Acid under Moist-Solid Conditions. *ACS Sustainable Chem. Eng.* **2023**, *11* (27), 9924–9931. https://doi.org/10.1021/acssuschemeng.2c06847.
(21) Zaker, A.; Auclair, K. Mechanoenzymatic Depolymerization of Polyethylene Terephthalate in Moist Solids: Exploring the Roller Mill. *ACS Sustainable Chem. Eng.* **2025**, *13* (21), 8093–8102. https://doi.org/10.1021/acssuschemeng.5c02335.
(22) Tricker, A. W.; Osibo, A. A.; Chang, Y.; Kang, J. X.; Ganesan, A.; Anglou, E.; Boukouvala, F.; Nair, S.; Jones, C. W.; Sievers, C. Stages and Kinetics of Mechanochemical Depolymerization of Poly(Ethylene Terephthalate) with Sodium Hydroxide. *ACS Sustainable Chem. Eng.* **2022**, *10* (34), 11338–11347. https://doi.org/10.1021/acssuschemeng.2c03376.
(23) Zeitler, S. M.; Chakma, P.; Golder, M. R. Diaryliodonium Salts Facilitate Metal-Free Mechanoredox Free Radical Polymerizations. *Chem. Sci.* **2022**, *13* (14), 4131–4138. https://doi.org/10.1039/D2SC00313A.
(24) Krusenbaum, A.; Grätz, S.; Tigineh, G. T.; Borchardt, L.; Kim, J. G. The Mechanochemical Synthesis of Polymers. *Chem. Soc. Rev.* **2022**, *51* (7), 2873–2905. https://doi.org/10.1039/D1CS01093J.
(25) Ohn, N.; Shin, J.; Kim, S. S.; Kim, J. G. Mechanochemical Ring-Opening Polymerization of Lactide: Liquid-Assisted Grinding for the Green Synthesis of Poly(Lactic Acid) with High Molecular Weight. *ChemSusChem* **2017**, *10* (18), 3529–3533. https://doi.org/10.1002/cssc.201700873.
(26) Hong, S.-J.; Jeong, H.; Yuk, J. S.; Park, M.; Kim, G.; Kim, Y.-W.; Shin, J. Semicrystalline-Glassy Multiblock Copolymers via Mechanochemical Synthesis toward Tough Poly(Lactide). *ACS Sustainable Chem. Eng.* **2022**, *10* (44), 14523–14538. https://doi.org/10.1021/acssuschemeng.2c04236.
(27) Skala, M. E.; Zeitler, S. M.; Golder, M. R. Liquid-Assisted Grinding Enables a Direct Mechanochemical Functionalization of Polystyrene Waste. *Chem. Sci.* **2024**, *15* (28), 10900–10907. https://doi.org/10.1039/D4SC03362K.
(28) Kim, G.; Park, B.; Kim, N.; Hwang, Y.-J.; Rizzo, A.; Peterson, G. I. Waste Polystyrene Upcycling via the Birch Reduction with Ball-Mill Grinding. *Nat Commun* **2025**, *16* (1), 5924. https://doi.org/10.1038/s41467-025-61119-z.
(29) Ardila‐Fierro, K. J.; Hernández, J. G. Sustainability Assessment of Mechanochemistry by Using the Twelve Principles of Green Chemistry. *ChemSusChem* **2021**, *14* (10), 2145–2162. https://doi.org/10.1002/cssc.202100478.
(30) Andersen, J.; Mack, J. Mechanochemistry and Organic Synthesis: From Mystical to Practical. *Green Chemistry* **2018**, *20* (7), 1435–1443. https://doi.org/10.1039/C7GC03797J.
(31) Lee, H. W.; Lee, J. Y.; Borchardt, L.; Kim, J. G. Catalyst- and Solvent-Free Depolymerization of Poly(Bisphenol A Carbonate): Aminolysis. *Green Chem.* **2025**, *27* (38), 11928–11935. https://doi.org/10.1039/D5GC03046C.
(32) Sanchez-Rexach, E.; Johnston, T. G.; Jehanno, C.; Sardon, H.; Nelson, A. Sustainable Materials and Chemical Processes for Additive Manufacturing. *Chem. Mater.* **2020**, *32* (17), 7105–7119. https://doi.org/10.1021/acs.chemmater.0c02008.
(33) Cha, S.; Kim, J. G.; Peterson, G. I. Influence of Crystallinity on the Mechanochemical Degradation of Poly(Lactide) with Ball-Mill Grinding. *Macromolecules* **2024**, *57* (21), 9960–9964. https://doi.org/10.1021/acs.macromol.4c02156.
(34) Pham, D. D.; Cho, J. Low-Energy Catalytic Methanolysis of Poly(Ethyleneterephthalate). *Green Chem.* **2021**, *23* (1), 511–525. https://doi.org/10.1039/D0GC03536J.
(35) Van Westrenen, J.; Chang, Y.; Nguyen, V. S.; Hepstall, A.; Gołąbek, K.; Schork, F. J.; Sievers, C. Effect of Polymer Structure and Material Properties on Mechanochemical Reaction Environments for Polymer Recycling. *Chem Circularity* **2026**, 100021. https://doi.org/10.1016/j.checir.2026.100021.
(36) Gołąbek, K.; Chang, Y.; Mellinger, L. R.; Rodrigues, M. V.; Nogueira, C. de S. C.; Passos, F. B.; Xing, Y.; Passos, A. R.; Saffarini, M. H.; Isner, A. B.; Sholl, D. S.; Sievers, C. Spatially Resolved Reaction Environments in Mechanochemical Upcycling of Polymers. *Chem* **2026**, *12* (1). https://doi.org/10.1016/j.chempr.2025.102754.
(37) Gołąbek, K.; Mellinger, L. R.; Bush, S. T.; Phillips, E. V.; Marinis, G. A.; Nguyen, V. S.; van Westrenen, J.; Sievers, C. Mechanochemical Depolymerization of PET: Kinetic Studies on Alkaline Hydrolysis of Commercial Feedstocks. *ChemSusChem* **2026**, *19* (3), e202502416. https://doi.org/10.1002/cssc.202502416.

View Article Online
DOI: 10.1039/D6PY00436A

(38) Westrenen, J. van; Chang, Y.; Nguyen, V. S.; Hepstall, A.; Gołąbek, K.; Schork, F. J.; Sievers, C. Effect of Polymer Structure and Material Properties on Mechanochemical Reaction Environments for Polymer Recycling. *Chem Circularity* **2026**, *0* (0). https://doi.org/10.1016/j.checir.2026.100021.
(39) Lee, H. W.; Lee, J. Y.; Borchardt, L.; Kim, J. G. Catalyst- and Solvent-Free Depolymerization of Poly(Bisphenol A Carbonate): Aminolysis. *Green Chem.* **2025**, *27* (38), 11928–11935. https://doi.org/10.1039/D5GC03046C.
(40) Boyandin, A. N.; Bessonova, V. A.; Ertiletskaya, N. L.; Sukhanova, A. A.; Shalygina, T. A.; Kondrasenko, A. A. Aminolysis of Poly-3-Hydroxybutyrate in N,N-Dimethylformamide and 1,4-Dioxane and Formation of Functionalized Oligomers. *Polymers* **2022**, *14* (24), 5481. https://doi.org/10.3390/polym14245481.
(41) Xia, Y.; Auclair, K. Mechanoenzymatic Depolymerization of Highly Crystalline Polyethylene Naphthalate under Moist-Solid Conditions. *ACS Sustainable Chem. Eng.* **2024**, *12* (40), 14832–14840. https://doi.org/10.1021/acssuschemeng.4c05734.
(42) Hasiweder, T. J.; Dinh, H. M.; Pandey, D. K.; Sorvanov, A.; Khusnutdinova, J. R. Mechanoactivated Celite as a Catalyst for C–H Bond Perfluoroalkylation and Other Radical Reactions. *Angewandte Chemie International Edition* **2025**, *64* (33), e202504137. https://doi.org/10.1002/anie.202504137.
(43) Machado, T. O.; Stubbs, C. J.; Chiaradia, V.; Alraddadi, M. A.; Brandolese, A.; Worch, J. C.; Dove, A. P. A Renewably Sourced, Circular Photopolymer Resin for Additive Manufacturing. *Nature* **2024**, *629* (8014), 1069–1074. https://doi.org/10.1038/s41586-024-07399-9.
(44) Wei, X.; Zhang, X.; Chen, T.; Huang, J.; Li, T.; Zhang, X.; Wang, S.; Dong, W. UV-Mediated Facile Fabrication of a Robust, Fully Renewable and Controllably Biodegradable Poly(Lactic Acid)-Based Covalent Adaptable Network. *ACS Macro Lett.* **2024**, *13* (9), 1112–1118. https://doi.org/10.1021/acsmacrolett.4c00377.
(45) Choi, C.; Okayama, Y.; Morris, P. T.; Robinson, L. L.; Gerst, M.; Speros, J. C.; Hawker, C. J.; Read de Alaniz, J.; Bates, C. M. Digital Light Processing of Dynamic Bottlebrush Materials. *Advanced Functional Materials* **2022**, *32* (25), 2200883. https://doi.org/10.1002/adfm.202200883.
(46) Choi, C.; Self, J. L.; Okayama, Y.; Levi, A. E.; Gerst, M.; Speros, J. C.; Hawker, C. J.; Read de Alaniz, J.; Bates, C. M. Light-Mediated Synthesis and Reprocessing of Dynamic Bottlebrush Elastomers under Ambient Conditions. *J. Am. Chem. Soc.* **2021**, *143* (26), 9866–9871. https://doi.org/10.1021/jacs.1c03686.
(47) Nelson, B. R.; Cione, J. T.; Kirkpatrick, B. E.; Kreienbrink, K. M.; Dhand, A. P.; Burdick, J. A.; Iv, C. W. S.; Anseth, K. S.; Bowman, C. N. Multifunctional Dithiolane Monomers for Multi-Scale, Recyclable Light-Driven Additive Manufacturing. *Polym. Chem.* **2025**, *16* (18), 2108–2116. https://doi.org/10.1039/D5PY00199D.
(48) Han, S.; Bobrin, V. A.; Michelas, M.; Hawker, C. J.; Boyer, C. Sustainable and Recyclable Acrylate Resins for Liquid-Crystal Display 3D Printing Based on Lipoic Acid. *ACS Macro Lett.* **2024**, *13* (11), 1495–1502. https://doi.org/10.1021/acsmacrolett.4c00600.
(49) Lee, D.; Wang, H.; Jiang, S.-Y.; Verduzco, R. Versatile Light-Mediated Synthesis of Degradable Bottlebrush Polymers Using α-Lipoic Acid. *Angewandte Chemie International Edition* **2024**, *63* (48), e202409323. https://doi.org/10.1002/anie.202409323.
(50) Michal, B. T.; Jaye, C. A.; Spencer, E. J.; Rowan, S. J. Inherently Photohealable and Thermal Shape-Memory Polydisulfide Networks. *ACS Macro Lett.* **2013**, *2* (8), 694–699. https://doi.org/10.1021/mz400318m.
(51) Shi, C.-Y.; Zhang, Q.; Wang, B.-S.; Chen, M.; Qu, D.-H. Intrinsically Photopolymerizable Dynamic Polymers Derived from a Natural Small Molecule. *ACS Appl. Mater. Interfaces* **2021**, *13* (37), 44860–44867. https://doi.org/10.1021/acsami.1c11679.
(52) Dikshit, K. V.; Visal, A. M.; Janssen, F.; Larsen, A.; Bruns, C. J. Pressure-Sensitive Supramolecular Adhesives Based on Lipoic Acid and Biofriendly Dynamic Cyclodextrin and Polyrotaxane Cross-Linkers. *ACS Appl. Mater. Interfaces* **2023**, *15* (13), 17256–17267. https://doi.org/10.1021/acsami.3c00927.
(53) Pal, S.; Shin, J.; DeFrates, K.; Arslan, M.; Dale, K.; Chen, H.; Ramirez, D.; Messersmith, P. B. Recyclable Surgical, Consumer, and Industrial Adhesives of Poly(α-Lipoic Acid). *Science* **2024**, *385* (6711), 877–883. https://doi.org/10.1126/science.ado6292.
(54) Lin, H.-Y.; Li, L.; Zhang, Q.; Qu, D.-H.; Tong, F. Robust Supramolecular Adhesives Based on Natural Small Molecules Through Hydrogen Bonding. *Chemistry – A European Journal* **2025**, *31* (26), e202500900. https://doi.org/10.1002/chem.202500900.

View Article Online
DOI: 10.1039/D6PY00436A

(55) Pal, S.; Salzman, E. E.; Ramirez, D.; Chen, H.; Perez, C. A.; Dale, K.; Ghosh, S. K.; Lin, L.; Messersmith, P. B. Versatile Solid-State Medical Superglue Precursors of α-Lipoic Acid. *J. Am. Chem. Soc.* **2025**, *147* (16), 13377–13384. https://doi.org/10.1021/jacs.4c18448.
(56) Albanese, K. R.; Okayama, Y.; Morris, P. T.; Gerst, M.; Gupta, R.; Speros, J. C.; Hawker, C. J.; Choi, C.; de Alaniz, J. R.; Bates, C. M. Building Tunable Degradation into High-Performance Poly(Acrylate) Pressure-Sensitive Adhesives. *ACS Macro Lett.* **2023**, *12* (6), 787–793. https://doi.org/10.1021/acsmacrolett.3c00204.
(57) Okayama, Y.; Morris, P.; Albanese, K.; Olsen, S.; Mori, A.; de Alaniz, J. R.; Bates, C. M.; Hawker, C. J. Enhanced Degradation of Vinyl Copolymers Based on Lipoic Acid. *Journal of Polymer Science n/a* (n/a). https://doi.org/10.1002/pol.20241085.
(58) Albanese, K. R.; Read de Alaniz, J.; Hawker, C. J.; Bates, C. M. From Health Supplement to Versatile Monomer: Radical Ring-Opening Polymerization and Depolymerization of *α*-Lipoic Acid. *Polymer* **2024**, *304*, 127167. https://doi.org/10.1016/j.polymer.2024.127167.
(59) Tsutsuba, T.; Tachibana, Y.; Shimizu, M.; Kasuya, K. Marine Biodegradation of Poly(Butylene Succinate) Incorporating Disulfide Bonds Triggered by a Switch Function in Response to Reductive Stimuli. *ACS Appl. Polym. Mater.* **2023**, *5* (4), 2964–2970. https://doi.org/10.1021/acsapm.3c00147.
(60) Kristensen, M. M.; Løvschall, K. B.; Zelikin, A. N. Mechanisms of Degradation for Polydisulfides: Main Chain Scission, Self-Immolation, Or Chain Transfer Depolymerization. *ACS Macro Lett.* **2023**, *12* (7), 955–960. https://doi.org/10.1021/acsmacrolett.3c00345.
(61) Chakma, P.; Konkolewicz, D. Dynamic Covalent Bonds in Polymeric Materials. *Angewandte Chemie International Edition* **2019**, *58* (29), 9682–9695. https://doi.org/10.1002/anie.201813525.
(62) Heiner, A. C.; Bishop, K. M.; Musgrave, G. M.; Huber, A. K.; Cushman, L. M.; Bates, J. S.; Wang, C. Soil Compostability of Ester-Based Thiol–Ene Photopolymer Networks. *ACS Sustainable Chem. Eng.* **2024**, *12* (24), 9067–9077. https://doi.org/10.1021/acssuschemeng.4c01018.
(63) Alraddadi, M. A.; Chiaradia, V.; Stubbs, C. J.; Worch, J. C.; Dove, A. P. Renewable and Recyclable Covalent Adaptable Networks Based on Bio-Derived Lipoic Acid. *Polym. Chem.* **2021**, *12* (40), 5796–5802. https://doi.org/10.1039/D1PY00754H.
(64) Sieredzinska, B.; Zhang, Q.; Berg, K. J. van den; Flapper, J.; Feringa, B. L. Photo-Crosslinking Polymers by Dynamic Covalent Disulfide Bonds. *Chem. Commun.* **2021**, *57* (77), 9838–9841. https://doi.org/10.1039/D1CC03648C.
(65) Hiemenz, P. C.; Lodge, T. P. *Polymer Chemistry*, 2nd ed.; CRC Press: Boca Raton, FL, 2007.
(66) Sun, M.; Felsenthal, L. M.; Kim, S.; Choi, E. Y.; Reed, L. J.; Elling, B. R.; Dichtel, W. R. Covalent Adaptable Networks: Reprocessable Cross-Linked Polymers. *Chem. Rev.* **2026**, *126* (3), 1829–1948. https://doi.org/10.1021/acs.chemrev.4c00994.
(67) Han, J.; Liu, T.; Hao, C.; Zhang, S.; Guo, B.; Zhang, J. A Catalyst-Free Epoxy Vitrimer System Based on Multifunctional Hyperbranched Polymer. *Macromolecules* **2018**, *51* (17), 6789–6799. https://doi.org/10.1021/acs.macromol.8b01424.
(68) Quinn, E. C.; Hamernik, L. J.; Law, J. N.; Clarke, R. W.; Milrod, M.; Kozarekar, S.; Mick, R. M.; Sobkowicz, M. J.; Broadbelt, L. J.; Knott, B. C.; Knauer, K. M. Cracking the Code of Multi-Layer Films to Promote Circularity in Single-Use Plastic Packaging. *Nat Commun* **2026**, *17* (1), 1489. https://doi.org/10.1038/s41467-026-68936-w.
(69) Cayirli, S. Influences of Operating Parameters on Dry Ball Mill Performance. *Physicochemical Problems of Mineral Processing; ISSN 2084-4735* **2018**. https://doi.org/10.5277/PPMP1876.
(70) Lin, C.; Hu, H.; Zhu, H.; Luan, Q.; Li, Z.; Wang, J.; Zhu, J. Disulfide-Driven On-Demand Degradation of the PBAT Copolymer: Stable Comprehensive Performance, Long-Term Storage, and Redox-Induced Degradation. *Macromolecules* **2025**, *58* (8), 4170–4182. https://doi.org/10.1021/acs.macromol.4c02244.
(71) Bolt, R. R. A.; Leitch, J. A.; Jones, A. C.; Nicholson, W. I.; Browne, D. L. Continuous Flow Mechanochemistry: Reactive Extrusion as an Enabling Technology in Organic Synthesis. *Chem. Soc. Rev.* **2022**, *51* (11), 4243–4260. https://doi.org/10.1039/D1CS00657F.
(72) Bolt, R. R. A.; Smallman, H. R.; Leitch, J. A.; Bluck, G. W.; Barreteau, F.; Iosub, A. V.; Constable, D.; Dapremont, O.; Richardson, P.; Browne, D. L. Solvent Minimized Synthesis of Amides by Reactive Extrusion. *Angewandte Chemie International Edition* **2024**, *63* (41), e202408315. https://doi.org/10.1002/anie.202408315.

View Article Online
DOI: 10.1039/D6PY00436A

(73) Cha, S.; Peterson, G. I. Interpreting Polymer Chain Scission in Planetary Ball Mills Using Kinematic Energy Metrics. *Macromolecules* **2025**, *58* (18), 9944–9951. https://doi.org/10.1021/acs.macromol.5c01985.
(74) Kondo, S.; Sasai, Y.; Hosaka, S.; Ishikawa, T.; Kuzuya, M. Kinetic Analysis of the Mechanolysis of Polymethylmethacrylate in the Course of Vibratory Ball Milling at Various Mechanical Energy. *Journal of Polymer Science Part A: Polymer Chemistry* **2004**, *42* (17), 4161–4167. https://doi.org/10.1002/pola.20245.
(75) Nwoye, E.; Floyd, K.; Batteas, J.; Felts, J. Experimental Quantification of Impact Force and Energy for Mechanical Activation in Vibratory Ball Mills. *RSC Mechanochem.* **2025**, *2* (6), 911–922. https://doi.org/10.1039/D5MR00059A.
(76) Jafter, O. F.; Lee, S.; Park, J.; Cabanetos, C.; Lungerich, D. Navigating Ball Mill Specifications for Theory-to-Practice Reproducibility in Mechanochemistry. *Angewandte Chemie International Edition n/a* (n/a), e202409731. https://doi.org/10.1002/anie.202409731.

View Article Online
DOI: 10.1039/D6PY00436A

The data supporting this article have been included as part of the Supplementary Information.